ELSEVIER

Journal of Nuclear Materials 283–287 (2000) 642–646

journal of nuclear materials

www.elsevier.nl/locate/jnucmat

Development of an oxide dispersion strengthened, reduced-activation steel for fusion energy

G.R. Romanoski *, L.L. Snead, R.L. Klueh, D.T. Hoelzer

Oak Ridge National Laboratory, Bldg. 4508, MS 6088, P.O. Box 2008, Oak Ridge, TN 37831-6008, USA

Abstract

A reduced-activation steel having a nominal chemical composition of Fe, 9% Cr, 2% W, 0.25% V, 0.1% Ta, and 0.1% C was mechanically alloyed with a fine dispersion of Y_2O_3 and TiO_2 to assess the potential for extending the elevated temperature limit of this alloy for structural applications. The total oxide dispersion content was varied from 0.25% to 1% and the molar ratio, TiO_2/Y_2O_3 from 0 to 2. An argon atomized 9Cr2WVTa steel powder was ball milled under vacuum, extruded at 1150°C to a 16 to 1 reduction in area, followed by a normalize and age heat treatment. Mechanical properties were assessed by elevated temperature tensile tests over the temperature range from room temperature to 800°C. Transmission electron microscopy revealed a favorable dispersion of the oxide particles. Oxide dispersion strengthening by mechanical alloying resulted in significant improvement in elevated temperature tensile strengths. Extended ball-milling times improved oxide dispersion, microstructural refinement, and mechanical properties.

1. Introduction

Ferritic/martensitic steels are being considered for fusion applications because of their excellent swelling resistance and thermal properties [1]. However, the use of high-chromium conventional Cr–Mo steels or reduced-activation Cr–W steels for fusion power plant first wall and blanket structure would limit the upper operating temperature from 550°C to 600°C. In addition to the limited upper operating temperature determined by the creep strength, another problem with these steels is the reduction of impact toughness (increase in the transition temperature and decrease in the upper-shelf energy in a Charpy test) caused by neutron irradiation below 400–450°C. Thus, the use of these steels would limit operations to a range of 400–600°C (at a maximum) [2].

Dispersion strengthening is the most likely approach to provide the increased creep strength required in ferritic/martensitic steels for higher operating temperatures. The low number density of relatively large precipitates developed in the conventional or reduced-activation steels cannot provide sufficient creep strength beyond 550–600°C [2]. One way to widen the operating temperature window is to raise the upper-temperature limit to 650°C or higher. This can be done and still maintain the advantages inherent in ferritic/martensitic steels (e.g., high thermal conductivity and low swelling) by using oxide dispersion strengthened (ODS) steels [2]. Elevated temperature strength of these steels is obtained through microstructures that contain a high density of Y_2O_3 or TiO_2 particles dispersed in a ferrite matrix.

The first ODS steels were non-transformable ferritic steels [3–11] based on 13% Cr–1.5% Mo [3–6] and 11–13% Cr–3%W [10] ferritic matrices with titania (TiO_2) and/or Y_2O_3 dispersions. Commercial manufacture of the steels involves mechanical alloying of rapidly solidified alloy and ultrafine oxide powders, followed by consolidation by hot extrusion, rolling or hot isostatic pressing. The products generally have very fine grain size (<1 μm) and high uniaxial creep rupture strengths. Such a microstructure would also be desired for fusion applications [11]. This investigation seeks to emulate the success of Ukai et al. [12–14] by employing a Y_2O_3–TiO_2

* Corresponding author. Tel.: +1-865 574 4838; fax: +1-865 576 8424.

E-mail address: romanoskigr@ornl.gov (G.R. Romanoski).

0022-3115/00/$ - see front matter
PII: S0022-3115(00)00137-9

composite oxide for dispersion strengthening a tempered martensite matrix for enhanced elevated temperature service.

2. Experimental procedure

2.1. Material

Two matrix alloys were produced as argon atomized ferritic steel powder. The chemical composition of the two alloys, designated LAF and LAFY, are given in Table 1. The target composition for alloy LAF was identical to the low activation ferritic steel developed by Klueh et al. [1]. The composition of alloy LAFY included 0.9% yttrium. These base alloys were blended with fine Y_2O_3 and TiO_2 powders having 25–35 nm mean particle size such that the total oxide content was varied from 0.25% to 1% and the molar ratio, TiO_2/Y_2O_3, from 0 to 2. The base metal plus oxide compositions produced in this investigation are given in Table 2.

2.2. Processing

A 500-gm quantity of the matrix alloy served as the basis for each alloy. Oxides were added and ball milled in a vacuum attriter mill for 24, 48, or 96 h according to Table 2. The milling speed was modulated to prevent powder agglomeration. The milled powders were then encapsulated in a 51-mm diameter stainless steel can. Powders were degassed under vacuum at 400°C and sealed. The canned powders were extruded at 1150°C through a 12.7-mm diameter die in one pass resulting in a 16:1 reduction in area. The heat treatment was: austenitize for 1 h at 1050°C/air cool followed by tempering for 1 h at 750°C/air cool.

2.3. Characterization

Tensile tests were performed under vacuum from room temperature to 700°C at a strain rate of 10^{-3} using SS-3 miniature tensile specimens machined parallel to the extrusion direction. Microstructural characterization of the alloys included optical microscopy, scanning electron microscopy and transmission electron microscopy of thin foils.

3. Results and discussion

An assessment of the extruded and heat treated alloys revealed a tempered martensite microstructure with grain size typically less than 5 μm. The tempered martensite microstructure is basically ferrite with a fine dispersion of precipitated carbides and oxides incorporated during mechanical alloying. The transmission electron micrographs shown in Figs. 1 and 2 exhibit a favorable dispersion of the oxide-strengthening particles with mean spacing on the order of 100 nm. As can be seen in Fig. 2, extended ball-milling times, i.e., 96 h, resulted in a more refined microstructure with extensive subgrain formation.

Tensile tests have been completed for alloys designated: RK (the conventionally processed alloy), LAF-20, LAF-3, LAF-3B, LAF-3C, LAFY-3C, LAF-5,

Table 1
Composition of matrix alloys (wt%)[a]

Alloy	Cr	C[b]	Mn	W	V	Ta	Si	Y	Fe
RK	8.5–9	0.1	0.45	2.0	0.025	0.07	0.2	0	Bal.
LAF	8.6	0.065	0.44	2.0	0.29	0.08	0.24	0	Bal.
LAFY	8.8	0.011	0.47	2.0	0.28	0.07	0.24	0.85	Bal.

[a] RK: conventionally processed ferritic steel powder by Klueh et al. [1]; LAF and LAFY: argon atomized ferritic steel powders/sieve size: (−100/+400).
[b] Additional C pick-up from ball-milling operation is typically 0.04 wt%/24 h.

Table 2
Composition matrix for ODS ferritic steels[a]

Oxide additions ($Y_2O_3 + TiO_2$) (wt%)	Molar ratio TiO_2/Y_2O_3			
	0	0.5	1	2
1.0	LAF-1^{24}	LAF-2^{24}	LAF-3^{24} LAF-$3B^{48}$ LAF-$3C^{96}$ LAFY-$3C^{96}$	LAF-4^{24}
0.5	LAF-5^{24} LAF-$5B^{48}$ LAF-$5C^{96}$	LAF-6^{24}	LAF-7^{24}	LAF-8^{24}
0.25	LAF-9^{24}	LAF-10^{24}	LAF-11^{24}	LAF-12^{24}
0.1	LAF-13^{24}	LAF-14^{24}	LAF-15^{24}	LAF-16^{24}

[a] Y_2O_3 and TiO_2 powders were 25–35 nm particle size. Alloys were ball milled for the duration specified by the superscript (h); LAF-20: as received powder/no ball milling.

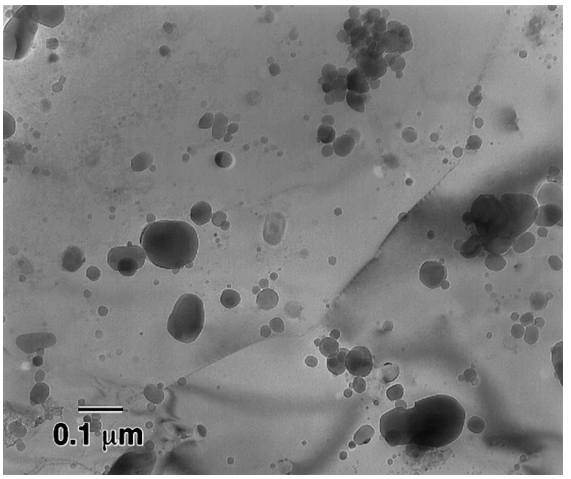

Fig. 1. Bright field transmission electron micrograph showing yttria particles dispersed in a ferritic steel matrix for alloy LAF-1. Ball-milling time was 24 h.

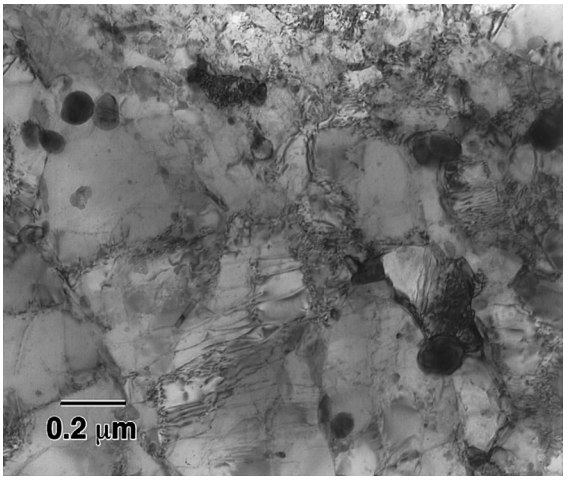

Fig. 2. Bright field electron micrograph showing yttria particles dispersed in a ferritic steel matrix with extensive subgrain formation for LAF-3. Ball-milling time was 96 h.

LAF-5B and LAF-5C. Engineering stress–strain curves are given in Fig. 3 for six alloys tested at 500°C. All OSD alloys exhibited a dramatically higher 0.2% offset yield strength and ultimate tensile strength compared to the conventionally processed base alloy of the same nominal composition. Total elongation values were typically 50% less for the ODS alloys. Maximum uniform elongation was not determined for the elevated temperature tests since stress relaxation may have been sufficient, at the slow testing rate, to change the shape of the stress–strain curve such that the peak load did not correspond to the onset of necking. Also evident in Fig. 3 is the dramatic effect of extended ball-milling times on improving the

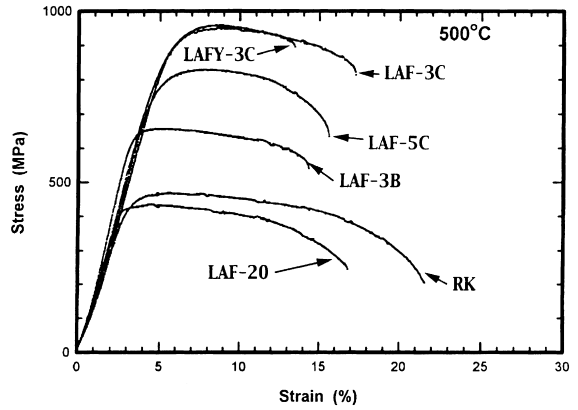

Fig. 3. Tensile stress–strain curves for six alloys tested at 500°C.

tensile properties. Alloy LAF-3B was milled for 48 h and is, consequently, weaker than LAF-3C and LAFY-3C (both milled for 96 h). Figs. 1 and 2 illustrate the additional microstructural refinement accomplished at the longer milling times. Apparently, the smaller subgrains remain stable at test temperatures and provide a sustained impediment to plastic deformation. This significant increase was accomplished without sacrificing ductility.

Alloy LAF-3C exhibited higher yield and ultimate strength compared to LAF-5C. It is not possible to offer a definitive explanation for the improved properties since the total oxide content of LAF-3C was greater than LAF-5C, and TiO_2 was also present in the stronger alloy. Total elongation was comparable. Additional tensile tests are being performed to survey the complete matrix of alloys produced for this investigation.

Stress–strain curves for alloy LAF-3C are given in Fig. 4 for temperatures ranging from room temperature to 700°C. The decrease in strength is generally attended

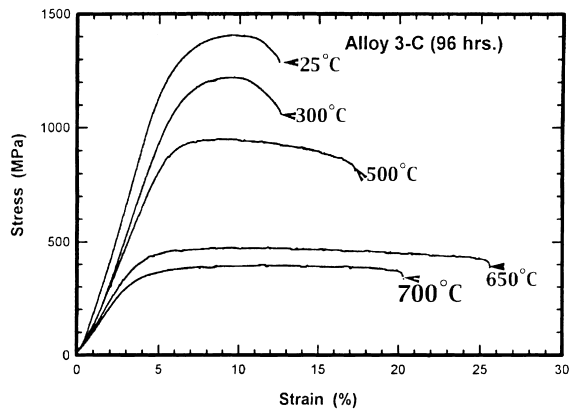

Fig. 4. Tensile stress–strain curves for alloy LAF-3C tested over the temperature range from room temperature to 700°C.

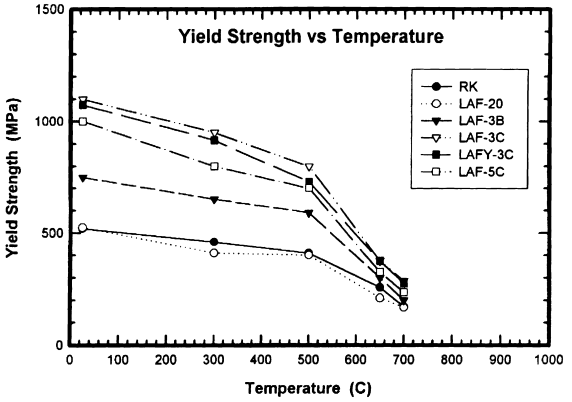

Fig. 5. Tensile yield strength versus temperature for six reduced-activation ferritic steels.

by an increase in ductility. The occurrence of stress relaxation is more evident at the intermediate temperatures, where both temperature and stress may be high enough for creep strain to cause some elastic unloading of the specimen.

A more comprehensive view of the effect of temperature on the yield and ultimate strength of these alloys is given in Figs. 5 and 6. The strongest ODS alloys produced, LAF-3C and LAFY-3C, maintain strengths a factor of two greater than the conventionally processed alloy over the full range of temperatures considered. A more pronounced decrease in strength with increasing temperatures is noted above 500°C. Above this temperature, carbide precipitation begins to degrade the strength of the alloy matrix. Resistance to plastic flow becomes more dependent on the dispersed oxide particles. Refinements to the microstructure such as the finer grain size likely contributed to the improvement in strength for the ODS alloys.

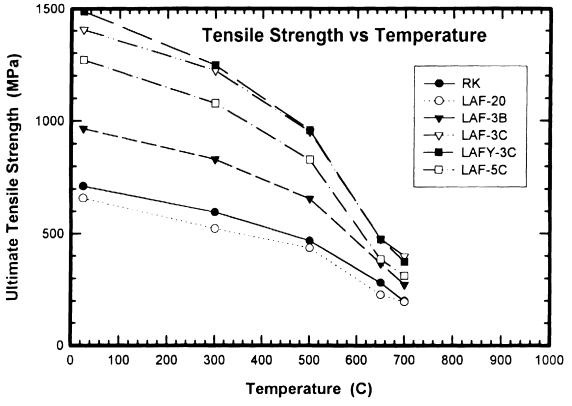

Fig. 6. Tensile ultimate strength versus temperature for six reduced-activation ferritic steels.

4. Conclusions

1. Oxide dispersion strengthening reduced-activation ferritic steels produced significant improvements in elevated temperature tensile strengths.
2. Extended ball-milling times improved oxide dispersion, microstructural refinement, and mechanical properties.

Acknowledgements

This research was sponsored in part by the Office of Fusion Energy Sciences, US Department of Energy under Contract No. DE-AC05-96OR22464 with Lockheed Martin Energy Research Corp. The authors are grateful to Jeff Bailey, Randy Howell, and Wade Jones for extensive experimental assistance.

References

[1] R.L. Klueh, K. Ehrlich, F. Abe, J. Nucl. Mater. 191–194 (1992) 116.
[2] A. Hishinuma, A. Kohyama, R. Klueh, D.S. Gelles, W. Dietz, K. Ehrlich, J. Nucl. Mater. 253–258 (1998) 193.
[3] M. Lippens, K. Ehrlich, V. Levy, C. Brown, A. Calza Bini, in: Proceedings of the International Conference on Materials for Nuclear Core Applications, vol. 1, BNES, London, 1987, p. 177.
[4] J.J. Huet, L. Coheur, L. De Wilde, J. Gedopt, W. Hendrix, W. Vandermeulen, in: J.W. Davis, D.J. Michel (Eds.), Proceedings of the Topical Conference on Ferritic Alloys for Use in Nuclear Energy Technologies, Met. Soc. AIME, Warrendale, PA, 1984, p. 329.
[5] J.J. Huet, L. Coheur, A. De Bremaeker, L. De Wilde, J.D. Gedopt, W. Hendrix, W. Vandermeulen, Nucl. Technol. 70 (1985) 215.
[6] L. De Wilde, J. Gedopt, S. De Burbure, A. Delbrassine, C. Driesen, B. Kazimierzak, in: Proceedings of the International Conference on Materials for Nuclear Core Applications, BNES, London, 1987, p. 271.
[7] A. Alamo, J. Decours, M. Pigoury, C. Foucher, in: Proceedings of the International Conference on Structural Applications of Machanical Alloying, American Society for Metals, Materials Park, OH, 1990, p. 89.
[8] S.D. Antolovich, R.W. Stusrud, R.A. Mackay, D.L. Anton, T. Khan, R.D. Kissinger, D.L. Klarstrom (Eds.), Superalloys 92, The Minerals, Metals, Materials Society, Warrendale, PA, 1992.
[9] A. Alamo, H. Regle, J.L. Bechade, Adv. Powder Metallurgy Particulate Mater. 7 (1992) 169.
[10] S. Ukai, M. Harada, M. Inoue, S. Nomura, S. Shikakura, M. Fujiwara, T. Nishida, K. Asabe, Trans. ANS 66 (1992) 186.
[11] D.M. Jaeger, A.R. Jones, in: D. Coutsouradis, J.H. Davidson, J. Ewald, P. Greenfield, T. Khan, M. Malik, D.B. Meadowcroft, V. Regis, R.B. Scarlin, F. Schubert,

D.V. Thorton (Eds.), Proceedings of the Conference on Materials for Advanced Power Engineering – Part II, Kluwer Academic, Dordrecht, 1994, p. 1507.
[12] S. Ukai, M. Harada, K. Okada, M. Inoue, S. Nomura, S. Shikakura, K. Asabe, T. Nishida, M. Fujiwara, J. Nucl. Mater. 204 (1993) 65.
[13] S. Ukai, T. Nishida, T. Okuda, T. Yoshitake, J. Nucl. Sci. Technol. 35 (1998) 294.
[14] S. Ukai, T. Nishida, H. Okada, M. Inoue, T. Okuda, M. Fujiwara, K. Asabe, in: Proceedings of the International Symposium on Material Chemistry in Nuclear Environment, Tsukuba, Japan, 14 & 15 March 1996, p. 891.